



Molecular steps for the syngas conversion on the Rh₆ cluster

Sharan Shetty^a, Rutger A. van Santen^a, Paul A. Stevens^b, Sumathy Raman^{b,*}

^a Schuit Institute of Catalysis, Eindhoven University of Technology, P.O. Box 513, 5600 MB Eindhoven, The Netherlands

^b ExxonMobil Research and Engineering, Annandale, NJ 08801, United States

ARTICLE INFO

Article history:

Received 24 March 2010

Received in revised form 9 June 2010

Accepted 1 July 2010

Available online 8 July 2010

Keywords:

Syngas
Metal cluster
Rh₆
DFT
Kinetics

ABSTRACT

In the present computational study, we investigate the competitive reaction pathways for the conversion of syngas to the formation of C₁ and C₂ oxygenated compounds such as formaldehyde, methanol, acetic acid, acetaldehyde and ethanol on a Rh₆ cluster. Moreover we also present pathways for the formation of methane and water, which are considered to be the major by-products in the syngas conversion. Our results demonstrate that the formation of the C₁ oxygenates takes place via the hydrogenation of the adsorbed CO molecule while the formation of C₂ oxygenates proceeds in two steps, i.e. CO dissociation to produce CH_x species followed by CO and/or HCO insertion.

An analysis obtained from the present calculations reveals that the product formation on Rh₆ cluster depends upon the CO:H₂ coverage. Under hydrogen rich conditions, the products will mainly consist of CH₃OH, CH₄ and water. The kinetic analysis based on rate constants obtained from harmonic transition state theory indicates that the initial step of CO hydrogenation is the rate-limiting step. Moreover, results suggest that the CO dissociation and the insertion steps for the formation of C₂ oxygenates on Rh₆ cluster have lower barriers compared to that on the Rh(1 1 1) surface.

© 2010 Elsevier B.V. All rights reserved.

1. Introduction

Fischer–Tropsch (F–T) mechanism provides an alternative route to produce liquid fuels via the catalytic conversion of syngas (CO + H₂) derived from natural gas, coal or biomass into olefins or paraffins and oxygenated compounds such as alcohols, ketones, aldehydes, acids, esters, etc. [1,2]. Although methane and water are the main by-products in the syngas conversion, the selectivity towards other compounds such as alkanes, alkenes and oxygenated compounds needs to be high [1–3]. Transition metals such as Ru, Co and Fe are suitable catalysts for the synthesis of long chain hydrocarbons such as paraffins or olefins [2–6]. On the other hand, Rh-based catalysts are better candidates for the formation of oxygenates such as alcohols, aldehydes and for the methanation reaction [7]. Among the oxygenated compounds, ethanol is considered as a promising alternative for fuel [3,8,9]. Studies have shown that the supported Rh-catalysts are highly selective for the formation of alcohols and aldehydes [10–13]. Recently, in a pioneering work Pan et al. have shown that the Rh–Mn nanoparticles confined inside carbon nanotube increase the overall formation of ethanol [14].

A low yield for the formation of ethanol is due to the molecular mechanism which involves the CO dissociation to create the CH_x species and the insertion of the undissociated CO molecule

in the CH_x species [3,15–17]. Hence, for a selective ethanol formation, it is necessary to find an optimum path which will create the CH_x species followed by the CO insertion. In the past, several mechanisms have been conjectured for the synthesis of C₁ and C₂ oxygenated compounds. Sachtler and Ichikawa have experimentally shown that CO insertion into surface–alkyl bonds creates acyl species, leading to oxygenates such as alcohols or aldehydes [15]. These studies have been carried out on SiO₂-supported Rh-catalysts in presence of promoters such as manganese or alkali ions. Choi and Liu have investigated the reaction path for the formation of ethanol on Rh(1 1 1) surface [18]. They proposed that the rate-limiting step in this process is to create the CH_x species followed by the CO insertion in the CH₃ species [18]. Recent experimental and theoretical studies have suggested that the yield towards oxygenated compounds can be increased by using promoters such as Mn [17]. The selectivity of the products produced on Rh clusters has also been controlled by the use of zeolites as a support. Rao et al., have shown that the encapsulated Rh clusters in zeolite Y act as active sites for the conversion of syngas to alcohols and hydrocarbons [19]. Gates et al. have extensively studied the role of carbonylated as well as decarbonylated Rh₆ clusters supported in NaY-zeolite in syngas conversion [12,20]. Their studies suggested that the zeolite plays a unique role in entrapping the Rh clusters and in increasing their selectivity.

Considering the significant role of Rh clusters in the formation of oxygenated compounds, mainly ethanol from the syngas, a detailed potential energy surface of syngas conversion on Rh₆

* Corresponding author.

E-mail address: sumathy.raman@exxonmobil.com (S. Raman).

cluster has been investigated. The competitive reaction pathways for various oxygenates formation and as well the paths for the formation of methane and water as by-products has been established. The manuscript deals with the following issues in the syngas conversion on Rh₆ cluster: (1) what are the competitive reaction pathways? (2) what is the rate-limiting step on small Rh clusters? (3) what are the intermediates which lead to the C₁ and C₂ oxygenated products? (4) how does the reaction pathway on Rh₆ cluster differs from that on the Rh surface?

2. Computational details

The calculations have been performed using a density functional approach with plane wave basis set in conjunction with projected augmented wave-functions (PAW) as implemented in the VASP code [21,22]. Spin polarized calculations were done using the generalized gradient approximation (GGA) with the PBE functional for the exchange correlation. All calculations have been carried out with clusters being placed in a cubic supercell maintaining a vacuum of 10 Å between the neighboring images. The calculations were restricted to the gamma point in the Brillouin zone sampling. The energy cut-off used for the plane wave was 400 eV. The energy was converged until the forces on the atoms were less than 0.05 eV/Å and the difference in energies between subsequent steps is less than 10⁻⁴ eV. The structures were optimized using the conjugate gradient technique. The reaction paths for the formation of C₁ and C₂ species and the diffusion of reaction intermediates have been generated by the nudged elastic band (NEB) as implemented in VASP [23]. In all pathways, twelve images have been generated between the initial and the final states using the interpolation method. Optimization of these images have been carried out using the steepest descent method. Transition states were characterized by the presence of only one imaginary frequency and rate constants were computed using the conventional harmonic oscillator transition state theory approximation [24]. Energies are reported after appropriate zero point energy corrections.

3. Results and discussions

This section is organized as follows: it begins with a discussion on the adsorption of C₁ and C₂ oxygenates studied in the present work, followed by a discussion on adsorption energies of CO in the presence of coadsorbed H and CO species. Subsequently, the results of CO hydrogenation and the formation of C₁ and C₂ oxygenated compounds have been summarized.

3.1. Adsorption of C₁ and C₂ oxygenates on Rh₆ cluster

The structures and adsorption energies of C₁ and C₂ oxygenates along with the CH₄ and H₂O molecules on the Rh₆ cluster are presented in Table 1. One can see that the CH₂O is strongly adsorbed relative to CH₃OH on the Rh₆ cluster implying that CH₂O can be a potential intermediate en route to other oxygenated compounds. In the case of C₂ oxygenates, the CH₃CHO is more strongly adsorbed in comparison to other C₂ oxygenates (Table 1). The stability of aldehydes on the Rh₆ cluster can be attributed to the π–σ-bond formed between the π of the C–O bond of aldehydes and σ of the Rh–Rh bond. The strong adsorption of aldehydes however indicate that they will be difficult to desorb compared to other oxygenates and hence are less likely to be the final product of syngas conversion on Rh₆ clusters.

The reader should refer to the supplementary information for a discussion on structural properties of the Rh₆ cluster and CO adsorption. In addition, efforts were also made to understand the effect of coadsorbed CO or H on the adsorption behaviour of CO

Table 1

Structures and the adsorption energies of C₁, C₂ oxygenated compounds, CH₄ and H₂O on Rh₆ cluster. Grey, yellow, red and blue spheres correspond to Rh, C, O and H atoms, respectively.

Adsorbed molecules	Structures	Adsorption energies (kJ/mol)
CH ₂ O		-157
CH ₃ OH		-47
CH ₃ CHO		-129
CH ₃ COOH		-59
CH ₃ CH ₂ OH		-51
CH ₄		-24
H ₂ O		-35

by investigating the structure and energetics of Rh₆(CO)_n (n = 1–3) and Rh₆(CO)_n(2H) (n = 1–3), Rh₆(CO)_n(4H) (n = 1, 2). Dissociatively adsorbed hydrogen atoms prefer a hollow or bridge site and never compete for the top-site on Rh₆ cluster. Results of CO adsorption energies are compiled in Table 2. As can be seen from Table 2, adsorption energies of CO are not influenced very strongly by the coadsorbed species. A top-site CO adsorption is always favored over a hollow site, and the adsorption energy of a top-site CO is ~210 kJ/mol.

3.2. Reaction pathways for the formation of C₁ oxygenates, CH_x intermediates and water

Scheme 1 (Fig. 1) represents the formation of CH_x (x = 0, 1, 2) intermediates, CH₂O and H₂O from the CO and 2H coadsorbed on the Rh₆ cluster, investigated in the present study.

Table 2Adsorption energies of CO in the presence of coadsorbed species. Top-site (t), hollow site (h), bridge (b) and geminal (gem) adsorption sites on the Rh₆ cluster are indicated.

Species	Reference state	1 st CO ads. energy (kJ/mol)	2 nd CO ads. energy (kJ/mol)	3 rd CO ads. energy (kJ/mol)
Rh ₆ (CO) ₂	Rh ₆ (CO)(t) + CO		-215(t) -207(h) -193(b)	
Rh ₆ (CO) ₃	Rh ₆ (CO) ₂ (tt) + CO			-202(t) -194(h) -181(b) -155(gem)
Rh ₆ (CO)(2H)	Rh ₆ (2H) + CO	-220(t) -193(h)		
Rh ₆ (CO)(4H)	Rh ₆ (4H) + CO	-210(t) -180(h)		
Rh ₆ (CO) ₂ (2H)	Rh ₆ (CO)(t)(2H) + CO		-210(t) -206(h) -194(b)	
Rh ₆ (CO) ₂ (4H)	Rh ₆ (CO)(t)(4H) + CO		-213(t) -191(h) -158(gem)	
Rh ₆ (CO) ₃ (2H)	Rh ₆ (CO) ₂ (th)(2H) + CO			-215(t) -191(h)

3.2.1. CO hydrogenation

In this section, the likely pathways for the hydrogenation of CO leading to the formation of CH₂O (as represented in Scheme 1) are discussed. The first step is the formation of COH intermediate via the hydrogenation of the CO in the top-site as shown in Table 3(a). In the transition state (TS) the H is attached to the C end and in the final state (FS) it moves to the O end forming the COH intermediate. The barrier to form COH through this path is 246 kJ/mol (Table 3(a)), which is higher than the desorption energy of CO, i.e. 220 kJ/mol (Fig. 2). This indicates that this path is unfavorable for the hydrogenation of CO to form COH; instead CO desorption will supersede. Alternative paths have also been considered for COH formation and it includes hydrogenation of CO adsorbed in the hollow site (Table 3(b)). The hydrogenation barrier along this path is 147 kJ/mol (Table 3(b)). This barrier is around 100 kJ/mol lower than the earlier path when the CO was adsorbed on a top-site. This is due to the differences in the TS structures of these paths. In the later path the H is not interacting with the C atom (Table 3(a)) and hence reduces the repulsive interaction between the H and the C. However, the formation of COH intermediate is endothermic in both the paths. The C–OH distance corresponds to 1.38 Å. This is about 0.16 Å stretched from the gas phase CO. Hence, one can consider this state to be a precursor for CO dissociation. Andersson et al. have shown that on Ni surfaces the CO dissociation proceeds through the COH intermediate [25]. The hydrogenation at the C end of the COH intermediate results in the hydroxymethylene (CHOH) intermediate

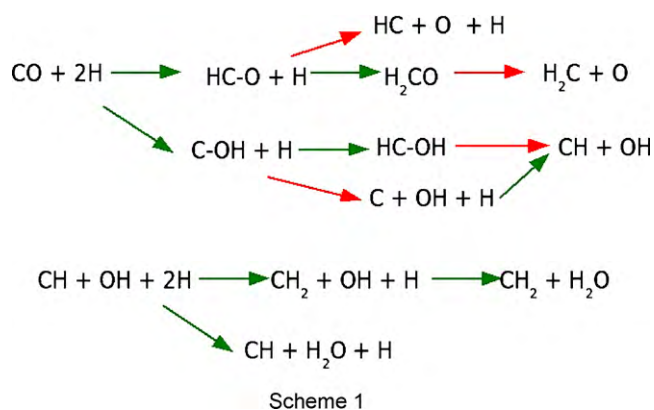


Fig. 1. Schematic representation of the reaction steps for the formation of C₁ intermediates. Green and red arrows represent the hydrogenation and C–O dissociation steps, respectively. (For interpretation of the references to color in the figure caption, the reader is referred to the web version of the article.)

(Table 3(c)) which requires a barrier of 102 kJ/mol. However, this intermediate is highly unstable with a reaction energy of 91 kJ/mol. The overall reaction barrier to form HCOH species from the CO and H coadsorbed state is about 244 kJ/mol (Fig. 2), which is above the desorption energy of CO. Hence, this path is less likely to occur on the Rh₆ cluster.

Having realized the difficulty in hydrogenation of CO at the oxygen end, efforts were made to establish the route to the formation of formyl (HCO) intermediate. Choi and Liu have suggested this step to be the rate-limiting step for the formation of methanol and ethanol with a barrier of 123 kJ/mol on Rh(1 1 1) surface [18]. The HCO intermediate can potentially adsorb in two different orientation. The HCO adsorbed in the top-site with C attached to the single Rh atom is highly unstable. The H atom moves back from the C atom to the Rh. This proves that the formation of the formyl intermediate is not possible when adsorbed perpendicular to the cluster. The strong repulsion between the CO and H is believed to be the cause of a higher barrier and is due to the loss in electron density on C as a result of the back donation to Rh₆ cluster [26]. The second possibility is the one wherein the C–O bond of HCO is parallel to the Rh–Rh bond as shown in Table 4(a). This state is more stable than the HCO on the top-site and the adsorbed COH intermediates. The reaction barrier corresponding to the formation of HCO is 88 kJ/mol (Table 4(a)), which is 59 kJ/mol lower than the formation of COH intermediate (Fig. 2). Moreover, the barrier to form HCO on Rh₆ cluster is 35 kJ/mol lower than that on the Rh(1 1 1) surface [18]. One can see that the barrier for the formation of HCO, which is considered to be the rate-limiting step on Rh(1 1 1) surface is substantially reduced on the Rh₆ cluster. The HCO intermediate is more stable than the COH intermediate largely due to the π–σ-interaction between the C–O bond and the Rh–Rh bond. Further hydrogenation of the HCO to form formaldehyde (CH₂O) is described in Table 4(b). This reaction barrier corresponds to 40 kJ/mol. However, this state is unstable by 35 kJ/mol. The desorption energy of CH₂O on Rh₆ cluster is 157 kJ/mol (Fig. 2). If we compare the formation of CH₂O on Rh(1 1 1) surface, the overall barrier on Rh₆ cluster is 113 kJ/mol, which is 25 kJ/mol lower than that on Rh(1 1 1) surface. This is due to the lowering of the barrier in the formation of HCO on Rh₆ cluster. The energy diagram represented in Fig. 2 suggests that the mono- and dihydrogenated carbonyl species are endothermic and can only be produced under non-trivial catalytic conditions such as high pressure in a hydrogen rich environment. The rate constants calculated at 300 K (Tables 3 and 4) suggest that the initial step for hydrogenation of CO is the formation of HCO intermediate.

Table 3
Structures of the reaction path, activation energy for the forward reaction, reaction energy, imaginary frequency of the transition state and the rate constants at 300 K for the formation of COH and HCOH intermediates on an Rh₆ cluster. Grey, yellow, red and blue spheres correspond to Rh, C, O and H atoms, respectively.

Initial state	Transition state	Final state	Activation energy (kJ/mol)	Reaction energy (kJ/mol)	Imaginary frequency (cm ⁻¹)	Rate constants at 300 K (s ⁻¹)
(a) CO(t) + 2H → COH(t) + H			246	196	1172	9.3 × 10 ⁻⁹
(b) CO(h) + 2H → COH(h) + H			147	112	1391	0.7
(c) COH(h) + 2H → HCOH(b) + H			102	91	327	1.98 × 10 ⁴

3.2.2. Formation of CH_x intermediates

The CO dissociation path seems to be the necessary step in the syngas conversion to generate the CH_x intermediate either to couple with another CH_x intermediate to form hydrocarbons

or to form oxygenated compounds via CO insertion. We initially considered the direct CO dissociation path on Rh₆ cluster without the assistance of H. In the FS the C and O ad-species distort the Rh₆ cluster and consequently increase the reaction energy

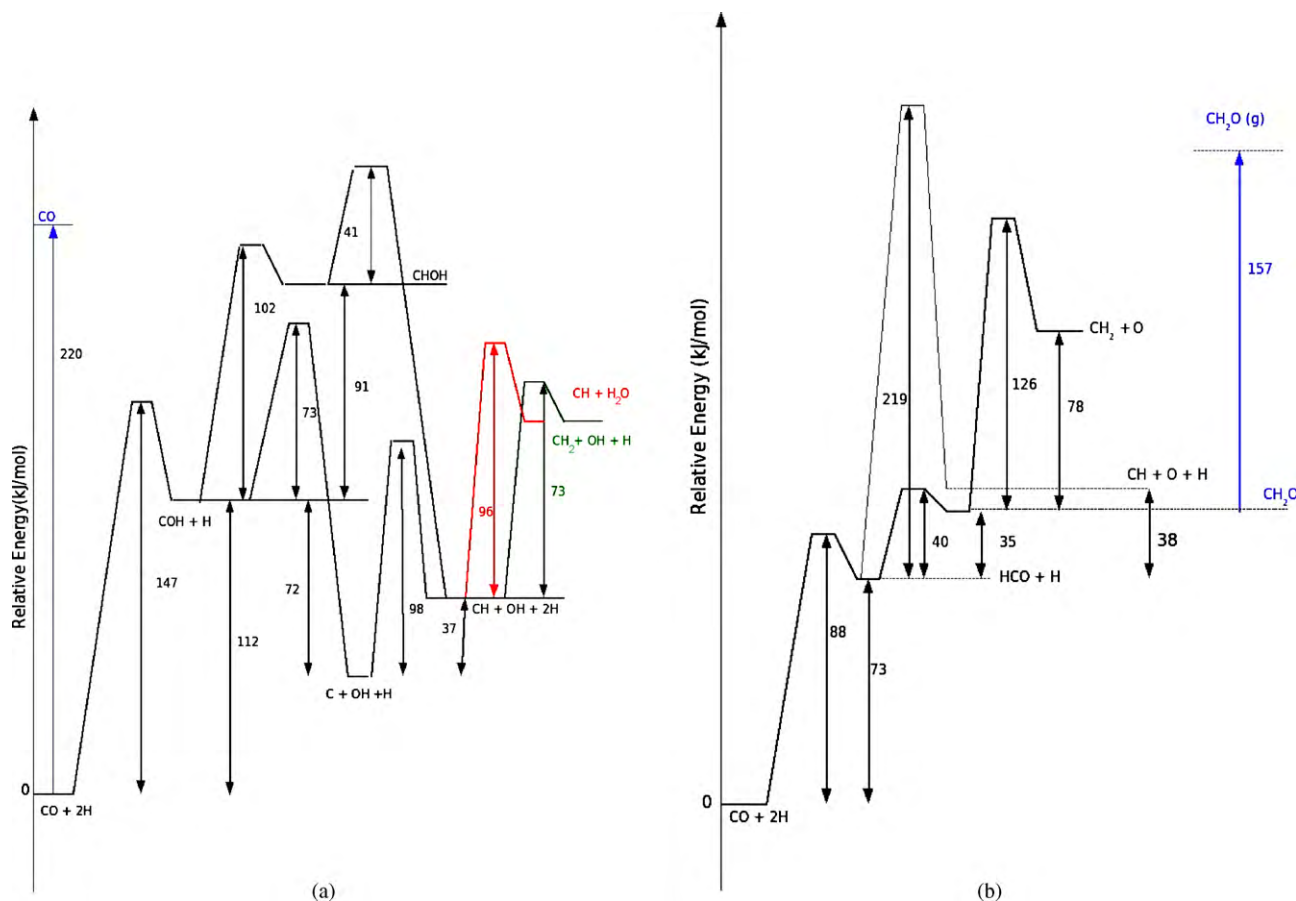

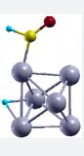
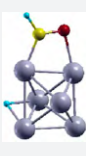

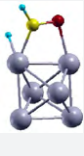



Fig. 2. Reaction paths for (a) formation of CH_x ($x=0, 1, 2$) species from the COH intermediate and (b) HCO intermediate. The desorption energies of CO and CH₂O (blue line) are given for comparison. The green and red lines in (a) show the further step to form CH₂ and H₂O, respectively. (For interpretation of the references to color in the figure caption, the reader is referred to the web version of the article.)

Table 4

Structures of the reaction path, activation energy for the forward reaction, the reaction energy, imaginary frequency of the transition state and the rate constants at 300 K for the formation of HCO and CH₂O intermediates on an Rh₆ cluster. Grey, yellow, red and blue spheres correspond to Rh, C, O and H atoms, respectively.

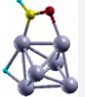

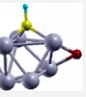

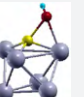


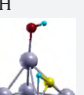

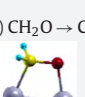
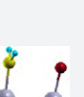
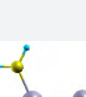
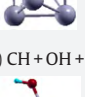
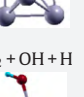

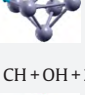
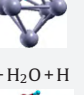

Initial state	Transition state	Final state	Activation energy (kJ/mol)	Reaction energy (kJ/mol)	Imaginary frequency (cm ⁻¹)	Rate constants at 300 K (s ⁻¹)
(a) CO (top) + 2H → HCO + H						
			88	73	176	1.0 × 10 ⁵
(b) HCO + H → CH ₂ O						
			40	35	597	9.5 × 10 ⁸

barrier by 157 kJ/mol. Since this energy is much higher than the hydrogenation steps discussed in the earlier section, this path has been discarded for generating the C₁ species. Moreover, the CO dissociation barrier reported on Rh(111) surface is around 350 kJ/mol which is much higher than the CO hydrogenation paths [18].

Subsequently, the formyl (HCO) intermediate is considered as a precursor state for generating the CH_x species via CO bond cleavage. The path is shown in Table 5(a). The CO dissociation barrier to form CH intermediate is found to be 219 kJ/mol and leading to an overall barrier of 292 kJ/mol with respect to CO and 2H (Fig. 2). This barrier is higher than the CO desorption which is 220 kJ/mol.

Table 5

Structures of the reaction path, activation energy for the forward reaction, the reaction energy, imaginary frequency of the transition state and the rate constants at 300 K for CO dissociation, CH and CH₂ formation on an Rh₆ cluster. Grey, yellow, red and blue spheres correspond to Rh, C, O and H atoms, respectively.

Initial state	Transition state	Final state	Activation energy (kJ/mol)	Reaction energy (kJ/mol)	Imaginary frequency (cm ⁻¹)	Rate constants at 300 K (s ⁻¹)
(a) HCO + H → HC + O + H						
			219	38	505	1.4 × 10 ⁻⁶
(b) COH (hollow) + H → C + OH + H						
			73	-72	292	1.1 × 10 ⁶
(c) C + OH + H → CH + OH						
			98	37	708	4.3 × 10 ⁴
(d) CH ₂ O → CH ₂ + O						
			126	78	183	107
(e) CH + OH + 2H → CH ₂ + OH + H						
			73	61	468	3.7 × 10 ⁷
(f) CH + OH + 2H → CH + H ₂ O + H						
			96	64	465	5.4 × 10 ⁵

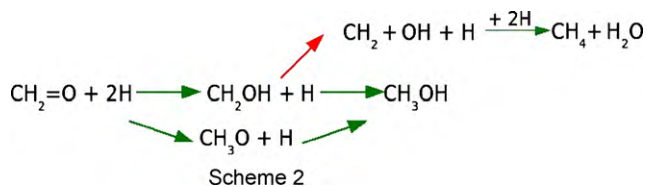


Fig. 3. Schematic representation of the reaction steps for the formation of CH_3OH and CH_4 . Green and red arrows represent the hydrogenation and C–O dissociation steps, respectively. (For interpretation of the references to color in the figure caption, the reader is referred to the web version of the article.)

The low rate constant of 1.4×10^{-6} for this reaction implies that the CO dissociation on Rh_6 cluster from the HCO intermediate is also improbable.

The CO dissociation path from the COH intermediate is shown in Table 5(b). The CO dissociation barrier corresponds to 73 kJ/mol and is exothermic by 72 kJ/mol with respect to the COH intermediate (Table 5(b)). This is due to the strong adsorption of C in the three-fold site. One can see that the CO bond cleavage from the COH intermediate has a lower barrier than from the HCO intermediate (Table 5(a) and (b)). This is due to the fact that the C–O bond is already stretched in the COH intermediate than in the HCO. The overall barrier to dissociate the CO bond via the COH interme-

diated with respect to the $\text{CO} + 2\text{H}$ coadsorbed state is 185 kJ/mol. The hydrogenation of the C atom to form the CH species has been described in Table 5(c). This step requires a barrier of 98 kJ/mol (Fig. 2).

The C–O bond cleavage from the CH_2O intermediate is 126 kJ/mol (Table 5(d)). The overall reaction barrier to dissociate from this intermediate with respect to CO and 2H is 239 kJ/mol (Fig. 2) suggesting an unfavorable C–O bond cleavage from CH_2O . Paths (e) and (f) in Table 5 correspond to the formation of CH_2 and H_2O , respectively. The barrier required for the formation of CH_2 is 23 kJ/mol lower than H_2O (Fig. 4).

In summary, both CH and CH_2 species can be easily formed via the CO dissociation of the COH intermediate. The results in Table 5 clearly suggest that the COH species once formed would lead to the formation of CH_x ($x=0, 1, 2$) species. The C–O bond in HCO and CH_2O intermediates are strong and would therefore prefer further hydrogenation over C–O dissociation.

3.2.3. Formation of methanol

Scheme 2 (Fig. 3) summarizes the reaction steps involved in further hydrogenation of the CH_2O towards the formation of methanol (CH_3OH) and methane (CH_4). We consider two possibilities for the hydrogenation of the CH_2O , i.e. at the C end to form the methoxy (CH_3O) species and the other at the O end to form the CH_2OH

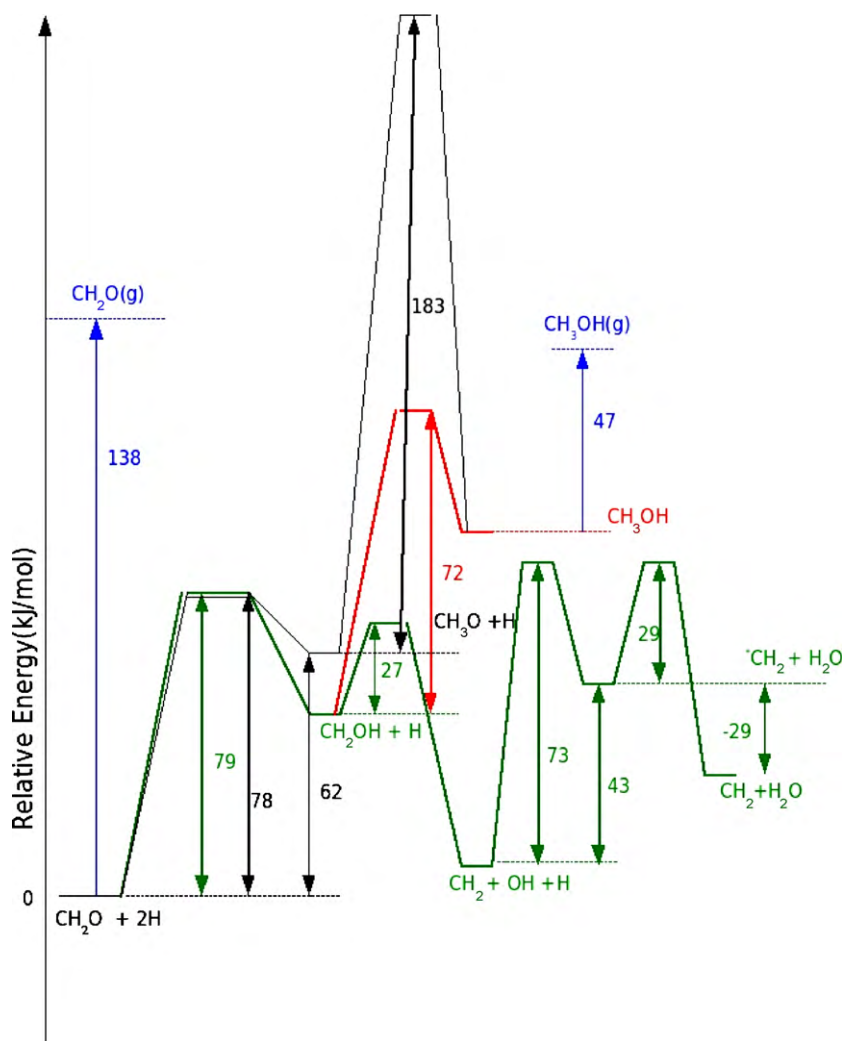



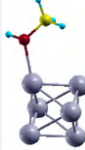
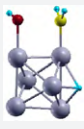



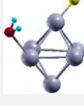
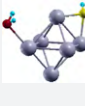


Fig. 4. Reaction path for the formation of CH_3OH (red and black lines) and CH_2 intermediate (green line) from the formaldehyde (CH_2O) intermediate. Blue line represents the desorption energies of CH_2O in the presence of 2H, and CH_3OH . (For interpretation of the references to color in the figure caption, the reader is referred to the web version of the article.)

Table 6

Structures of the reaction path, activation energy for the forward reaction, the reaction energy, imaginary frequency of the transition state and the rate constants at 300 K for the formation of (a) CH₂OH (b) CH₃OH, (c) CH₂ (d) formation of H₂O (e) diffusion of CH₂ from top to bridge. Grey, yellow, red and blue spheres correspond to Rh, C, O and H atoms, respectively.

Initial state	Transition state	Final state	Activation energy (kJ/mol)	Reaction energy (kJ/mol)	Imaginary frequency (cm ⁻¹)	Rate constants at 300 K (s ⁻¹)
(a) CH ₂ O + 2H → CH ₂ OH + H			79	45	996	2.7 × 10 ⁴
(b) CH ₂ OH + H → CH ₃ OH			72	45	274	1.3 × 10 ⁶
(c) CH ₂ OH + H → CH ₂ (top) + OH + H			27	-33	156	7.2 × 10 ¹⁰
(d) CH ₂ (top) + OH + H → CH ₂ (top) + H ₂ O			73	43	406	2.0 × 10 ⁶
(e) CH ₂ (top) + H ₂ O → CH ₂ (bridge) + H ₂ O			29	-29	171	1.0 × 10 ¹⁰

species as described in Table 6(a). It should be noted that in this path we increase the H concentration by co-adsorbing two hydrogen atoms. Its worth to mention that the adsorption energy of CH₂O decreases by 21 kJ/mol in presence of 2 coadsorbed H atoms (Fig. 4), as compared to a single CH₂O (Fig. 2(b)). This is due to the lateral interaction between the H atoms and the CH₂O on the Rh₆ cluster, suggesting that an increase in the H concentration on the Rh₆ cluster could decrease the desorption of the CH₂O. The barrier is of similar magnitude for both O- and C-hydrogenation and it amounts to 79 kJ/mol (Fig. 4), which is lower than the CO dissociation path from formaldehyde as described in Fig. 2(b). Hydrogenation of CH₂OH at the C end resulting into CH₃OH proceeds through the bridge H moving towards the C end as shown in Table 6(b). The bulkier CH₃ group moves away from the Rh atom due to the steric hindrance. The formation of methanol from CH₂OH has a barrier of 72 kJ/mol (Fig. 4) and the desorption energy of methanol is 47 kJ/mol. The formation of methanol through the methoxy (CH₃O) intermediate is unfavorable as seen in Fig. 4. The hydrogenation step to form CH₃OH from the methoxy intermediate requires a barrier of 183 kJ/mol. Hence this route has been discarded as a possible route to form methanol. This indicates that methanol formation takes place via the CH₂OH intermediate on Rh₆ cluster. This path is different than the one shown on Rh(111) surface by Choi and Liu [18]. They proposed the formation of methanol via the CH₃O intermediate.


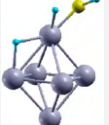
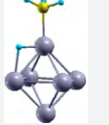

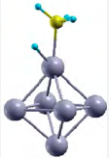
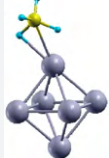
The other competitive path for CH_x formation is the CO bond cleavage from the CH₂OH intermediate to form the CH₂ and OH ad-species. This path is shown in Table 6(c). The barrier required

for the CO bond cleavage is 27 kJ/mol, and is 33 kJ/mol exothermic with respect to the CH₂OH intermediate. The OH can be eliminated through the formation of water with a barrier of 73 kJ/mol (Table 6(d)). The CH₂ species diffuses to a more stable bridge site with a barrier of 29 kJ/mol (Table 6(e)). In the earlier section, it was shown that the CO dissociation from the CH₂O intermediate was energetically unfavorable compared to its hydrogenation. The overall barrier for CO bond cleavage from the CH₂OH is 180 kJ/mol. This is similar to the overall barrier which has been proposed earlier along the COH intermediate. One should note that these barriers to create the CH_x species are much lower than that on the Rh(111) surface where the overall barriers are more than 200 kJ/mol from the coadsorbed CO + H [18]. The maximum rate required for the formation of CH₂ (bridge) and H₂O from CH₂OH is 2.0 × 10⁶ s⁻¹ on the Rh₆ cluster. Interestingly, this is similar to the rate to form CH₃OH, which is 1.3 × 10⁶ s⁻¹ (Table 6). This clearly implies that the formation of CH₃OH species is kinetically a possible route on the Rh₆ cluster.

3.2.4. Formation of methane

Since H₂O will be a spectator species in the formation of CH₄ we neglect its coadsorption on the cluster. The path for the formation of CH₃ from CH₂ and coadsorbed H is shown in Table 7(a). During the reaction, the CH₂ moves out of the bridge site and is hydrogenated from the neighboring bridge H to form CH₃. This reaction is exothermic by 33 kJ/mol. This is followed by the last addition of H to CH₃ to form CH₄ as shown in Table 7(b). This path has a barrier of 39 kJ/mol. The reaction path for the formation of CH₄ from the

Table 7
Structures of the reaction path, activation energy for the forward reaction, the reaction energy, imaginary frequency of the transition state and the rate constants at 300 K for the formation of (a) CH₃ (b) CH₄. Grey, yellow, blue spheres correspond to Rh, C and H atoms, respectively.

Initial state	Transition state	Final state	Activation energy (kJ/mol)	Reaction energy (kJ/mol)	Imaginary frequency (cm ⁻¹)	Rate constants at 300 K (s ⁻¹)
(a) CH ₂ + 2H → CH ₃ + H						
			57	-33	697	1.9 × 10 ⁸
(b) CH ₃ + H → CH ₄						
			39	18	782	1.3 × 10 ⁹

CH₂ intermediate is shown in Fig. 5. We can see that once the CH₂ intermediate is formed it can be easily hydrogenated to form CH₄ (Fig. 5). The desorption energy of methane is 24 kJ/mol. This clearly indicates that the CH₂OH is an important intermediate for the formation of methanol and methane on the Rh₆ cluster, especially under hydrogen rich conditions.

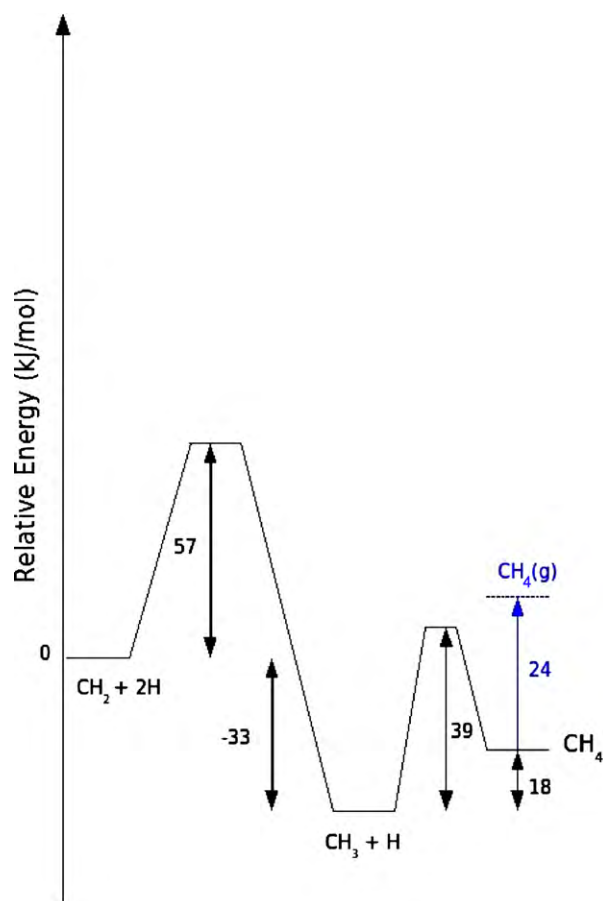


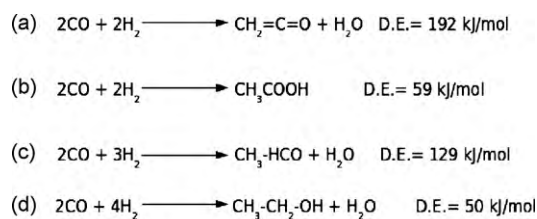
Fig. 5. Reaction pathway for the formation of CH₄ from CH₂ intermediate. The desorption energy of CH₄ (blue line) is given for comparison. (For interpretation of the references to color in the figure caption, the reader is referred to the web version of the article.)

3.3. Reaction pathways for the formation of C₂ oxygenates

Scheme 3 (Fig. 6) summarizes the reaction paths for the formation of C₂ oxygenates investigated in the present work. Reaction paths involving the coupling of CH_x with CH_x (x = 1, 3) or HCOH are not considered due to substantial overall barrier for the CO bond cleavage which is around 180 kJ/mol. In Scheme 3 the reactions have been presented considering the ratio of CO:H₂ as 1:1, 1:1.5 and 1:2. In a high coverage of CO there can be a possibility of the formation of CO₂ through the water-gas shift reaction. However, this path is not relevant for the present study and will not be discussed in this work. One should note that in a hydrogen rich environment, methane formation will dominate in comparison to any C₂ formation, based on our above investigation on C₁ intermediates. This is in agreement with the recent results on the ethanol formation on Rh(1 1 1) surface [18].

3.3.1. Formation of ketene and acetyl

Several studies have suggested that the route towards the formation of ethanol is either via the ketene (CH₂CO) or acetyl (CH₃CO) intermediate formed from the CO insertion in the CH₂ and CH₃, respectively [15,16]. The reaction mechanism for the CO insertion in CH₂ and CH₃ species is presented in Table 8(a) and (b), respectively. For the CO insertion in the CH₂ the barrier correspond to 108 kJ/mol (Fig. 7(a)). In the TS the CO molecule bends along the Rh–Rh bond, and in the FS the CO is parallel to the Rh–Rh bond. This allows a stable interaction of the π-bond of CO with the Rh–Rh σ bond. In a hydrogen rich environment, CH₂ would prefer further hydrogenation to CH₄ (involving a barrier of 57 kJ/mol) as opposed to CO insertion. Furthermore, the barrier for CO insertion to CH₃ to form acetyl intermediate (73 kJ/mol) is lower than ketene for-

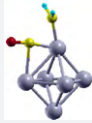
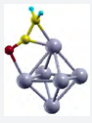
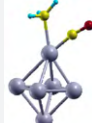
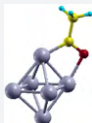
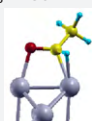

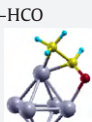
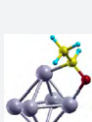
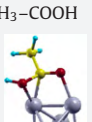
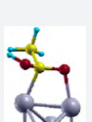


Scheme 3

Fig. 6. Scheme 3 shows the formation of C₂ oxygenates (a) ketene, (b) acetic acid (c) acetaldehyde and (d) ethanol on an Rh₆ cluster. The desorption energy (D.E.) of the stable C₂ oxygenates on an Rh₆ clusters are given.

Table 8

Structures of the reaction path, activation energy for the forward reaction, the reaction energy, imaginary frequency of the transition state and the rate constants at 300 K for ketene, acetaldehyde and acetic acid formation on an Rh₆ cluster. Grey, yellow, red and blue spheres correspond to Rh, C, O and H atoms, respectively.

Initial state	Transition state	Final state	Activation energy (kJ/mol)	Reaction energy (kJ/mol)	Imaginary frequency (cm ⁻¹)	Rate constants at 300 K (s ⁻¹)
(a) CO + CH ₂ → CH ₂ -CO			108	-0.2	451	9.7 × 10 ³
(b) CO + CH ₃ → CH ₃ -CO			73	36	259	5.1 × 10 ⁶
(c) CH ₃ -CO + H → CH ₃ -HCO			66	50	113	2.5 × 10 ⁷
(d) CH ₃ + HCO → CH ₃ -HCO			53	-20	422	1.7 × 10 ⁸
(e) CH ₃ -CO + OH → CH ₃ -COOH			115	93	95	965

mation (Fig. 7(b)) suggesting a low selectivity towards ketene and a less probable intermediate for the formation of ethanol or other oxygenated compounds. On the other hand the CO insertion in the CH₃ intermediate is 73 kJ/mol which is about 35 kJ/mol less than the ketene formation (Fig. 7). Moreover, the calculated rate constants suggest that the CH₃CO is much more easily formed than the CH₂CO intermediate (Table 8(a) and (b)). Hence, we suggest CH₃CO as one of the favorable intermediates for the formation of C₂ oxygenated compounds. Interestingly the barrier for CO insertion in CH₃ on the Rh(1 1 1) surface was shown to be 111 kJ/mol [18]. This is 38 kJ/mol higher than that on the Rh₆ cluster calculated by us.

3.3.2. Formation of acetaldehyde

Two potential reaction pathways were considered for acetaldehyde (CH₃-HCO) formation. It involves (a) insertion of CO to CH₃ followed by hydrogenation of the C end, and (b) hydrogenation of CO to form the formyl group followed by methylation of the formyl group. The CH₃CO can undergo hydrogenation to form CH₃-HCO, as shown in Table 8(c). The reaction barrier is 66 kJ/mol. The desorption energy of the acetaldehyde corresponds to 129 kJ/mol (Fig. 7(b)). The other competitive reaction to the formation of acetaldehyde is the CH₃ insertion in the HCO intermediate as shown in Table 8(d). Interestingly one can see that this has only a barrier of 53 kJ/mol. This is lower than the CO insertion in the CH₃ (Fig. 9). However, the overall barrier for the CH₃ insertion in the HCO intermediate from the coadsorbed CO and H is 126 kJ/mol as shown in Fig. 7(b). This is due to the endothermic state of the HCO intermediate. This suggests that the formation

of acetaldehyde is from the former route, i.e. CH₃ addition to CO followed by hydrogenation of the C end. The hydrogenation of the CH₃CO intermediate at the O end is endothermic by 122 kJ/mol. Hence we disregard this as a competitive reaction path for the formation of acetaldehyde.

3.3.3. Formation of acetic acid

We have shown in the above discussion that the formation of an acetyl group through the insertion of CO in the CH₃ group is a possible path for the formation of oxygenated compounds. Consequently, we investigated the path for the formation of acetic acid (CH₃COOH) from the acetyl intermediate. The path is shown in Table 8(e). The barrier for the insertion of the OH group in the acetyl intermediate has a barrier of 115 kJ/mol. However, the overall barrier to form acetic acid from the coadsorbed CH₃, CO and OH would be 151 kJ/mol (Fig. 7(b)). This shows that the acetic acid is also one of the possible C₂ oxygenates that could be formed on Rh₆ cluster. One should note that rate constants obtained for the formation of acetic acid and acetaldehyde at 300 K clearly indicate that the formation of acetaldehyde would be more favorable compared to the formation of acetic acid (Table 8). This agrees with the experimental interpretation by Sachtler and Ichikawa [15].

3.3.4. Formation of ethanol

Since the desorption energy of molecular hydrogen or the associative desorption energy of H₂ is quite low, it is less likely to have a high coverage on Rh₆ cluster. Consequently, acetaldehyde or acetic acid is less likely to be an intermediate involved in ethanol forma-

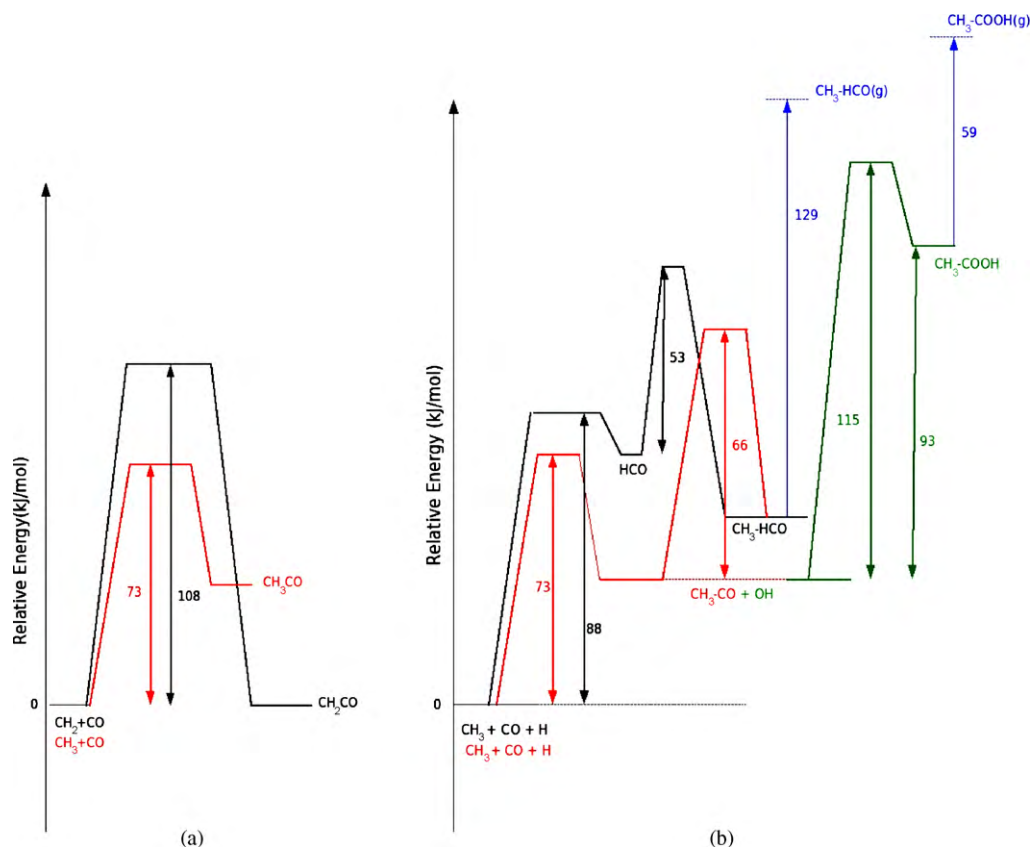
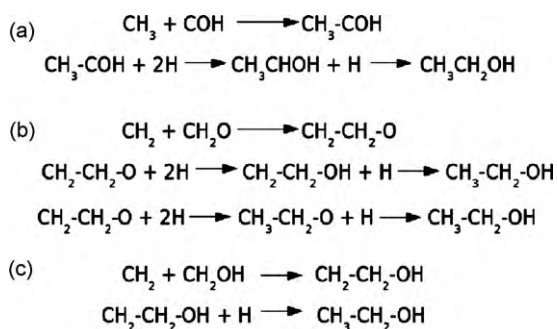


Fig. 7. Reaction path for the (a) insertion of CO in CH₂ (black line) and CH₃ (red line), (b) formation of acetaldehyde via the insertion of CH₃ in CO (red line) and HCO intermediate (black line) and the formation of acetic acid via the insertion of an OH group in the acetyl intermediate (green line). The desorption energy of acetaldehyde and acetic acid are shown in blue line. (For interpretation of the references to color in the figure caption, the reader is referred to the web version of the article.)

tion and so the hydrogenation pathways of acetaldehyde or acetic acid leading to ethanol have not been considered. Moreover, Wang et al. have shown from the experimental data that the formation of acetaldehyde and ethanol proceeds through different intermediates [13]. In an environment of high coverage of CO, we expect the partially hydrogenated carbonyls viz., C–OH, CH₂O, CH₂OH to be the potential reactive intermediates leading to ethanol as presented in Scheme 4 (Fig. 8).

Since further hydrogenation of C–OH to form HCOH involves an overall barrier of 244 kJ/mol, the insertion of CH_x may be a preferred path. Consequently, we examined the possibility of CH, CH₂ and CH₃ insertion to COH form C₂ oxygenates. Table 9 shows the mechanisms for the C–C coupling reactions through these paths. The CH₃ insertion in the COH group is only 61 kJ/mol. This is about




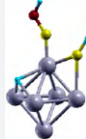
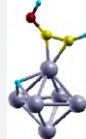
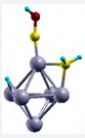
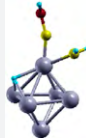

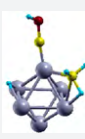
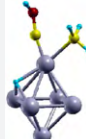
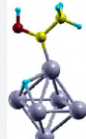
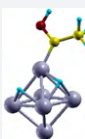
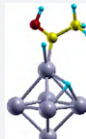



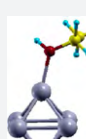
Scheme 4

Figure 8. Scheme 4 shows three different paths for the formation of ethanol (a) CH₃ + COH (b) CH₂ + CH₂O and (c) CH₂ + CH₂OH.

164 and 84 kJ/mol lower than the CH and CH₂ insertion paths, respectively. One can notice that as the CH group gets bulkier, the insertion in the COH is more favorable. This is due to the weak Rh–C bond as the CH group becomes bulkier. This was also observed in the earlier path (Table 8) where the CO insertion in the CH₃ intermediate was easier than in the CH₂ intermediate. Furthermore, the barrier for C–O dissociation from C–OH (73 kJ/mol) is higher than the CH₃ insertion barrier. These results suggest that CH₃ insertion in the COH intermediate would lead to the formation of ethanol. One should note that the barrier for the CH₃ insertion to C–OH is lower than the barrier for its insertion to CO. However, the barrier for COH formation from CO and 2H is higher, and therefore, in high CO coverage it would compete with acetaldehyde and acetic acid formation. Since the calculated barrier height for the hydrogenation of CH₃ to form methane is 57 kJ/mol, which is lower than the barrier for the insertion of CH₃ to COH (61 kJ/mol), in a high coverage H environment ethanol formation would compete with methane formation. We believe that the later path would be more favored based on barrier heights presented in Fig. 9(a).

The further reaction steps to form ethanol from the CH₃COH and 2H are shown in Table 9(d) and (e). The first hydrogenation step requires only 35 kJ/mol. The second hydrogenation with a barrier of 69 kJ/mol proceeds to form ethanol. The overall reaction barrier from the coadsorbed CH₃, COH and 2H is 78 kJ/mol (Fig. 9(a) and (b)). This low barrier for the formation of ethanol can be attributed to the stable products formed from the CH₃ insertion in COH (Fig. 9). Other competitive reactions for the formation of ethanol are presented in Tables 10 and 11. The path in Table 10 corresponds to the CH₂ insertion in the CH₂O and CH₂OH stable intermediates. The CH₂ insertion in the formaldehyde shows a lower barrier

Table 9
Structures of the reaction path, activation energy for the forward reaction, the reaction energy, imaginary frequency of the transition state and the rate constants at 300 K for CH_x ($x = 1, 2$ and 3) in the COH intermediate and formation of ethanol from COH on an Rh_6 cluster. Grey, yellow, red and blue spheres correspond to Rh, C, O and H atoms, respectively.

Initial state	Transition state	Final state	Activation energy (kJ/mol)	Reaction energy (kJ/mol)	Imaginary frequency (cm^{-1})	Rate constants at 300 K (s^{-1})	
(a) $\text{CH} + \text{COH} \rightarrow \text{CH-COH}$				225	-35	572	9.5×10^{-5}
(b) $\text{CH}_2 + \text{COH} \rightarrow \text{CH}_2\text{-COH}$				145	-22	604	1.9
(c) $\text{CH}_3 + \text{COH} \rightarrow \text{CH}_3\text{-COH}$				61	-36	100	5.2×10^7
(d) $\text{CH}_3\text{-COH} + 2\text{H} \rightarrow \text{CH}_3\text{-CHOH} + \text{H}$				35	8	746	2.3×10^9
(e) $\text{CH}_3\text{-CHOH} + \text{H} \rightarrow \text{CH}_3\text{-CH}_2\text{-OH}$				69	44	678	2.0×10^7

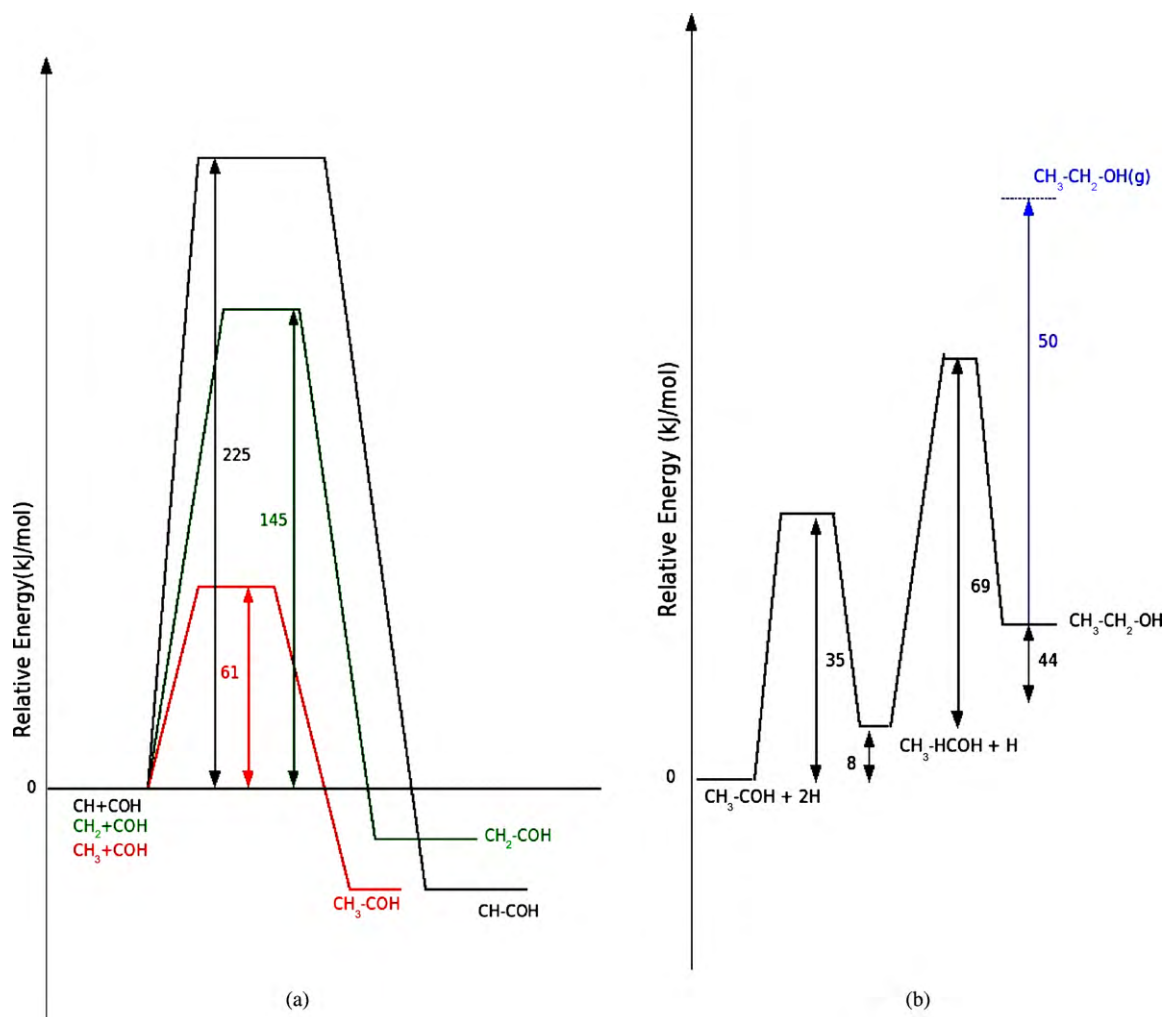


Fig. 9. (a) Reaction path for the insertion of CH (black line), CH₂ (green line) and CH₃ (red line) in the COH intermediate. (b) Reaction pathways for the formation of ethanol (CH₃CH₂OH). The desorption energy of ethanol is shown in blue line. (For interpretation of the references to color in the figure caption, the reader is referred to the web version of the article.)

than the CH₂OH intermediate (Fig. 10(a)). Hence, we consider the reaction steps of further hydrogenating the CH₂-CH₂-O intermediate to form ethanol. We initially hydrogenate the oxygen of the CH₂-CH₂-O intermediate to form CH₂-CH₂-OH (Table 11a). This step requires 35 kJ/mol and is exothermic. The hydrogenation of

the CH₂ end of this intermediate gives CH₃-CH₂-OH with a barrier of 60 kJ/mol as shown in Fig. 10(b). The other alternative path is to initially hydrogenate the CH₂ end to form ethoxy intermediate (Table 11(c)). This path is 27 kJ/mol higher than the earlier initial path (Table 11a). Moreover, the hydrogenation barrier of

Table 10

Structures of the reaction path, activation energy for the forward reaction, the reaction energy, imaginary frequency of the transition state and the rate constants at 300 K for (a) CH₂ insertion in CH₂O and (b) CH₂ insertion in CH₂OH on an Rh₆ cluster. Grey, yellow, red and blue spheres correspond to Rh, C, O and H atoms, respectively.

Initial state	Transition state	Final state	Activation energy (kJ/mol)	Reaction energy (kJ/mol)	Imaginary frequency (cm ⁻¹)	Rate constants at 300 K (s ⁻¹)
(a) CH ₂ + CH ₂ O → CH ₂ -CH ₂ O						
			98	-19	238	9.4 × 10 ⁴
(b) CH ₂ + CH ₂ OH → CH ₂ -CH ₂ OH						
			108	-22	66	5.5 × 10 ³

Table 11
Structures of the reaction path, activation energy for the forward reaction, the reaction energy, imaginary frequency of the transition state and the rate constants at 300 K for the formation of ethanol from $\text{CH}_2\text{-CH}_2\text{-O}$ and $\text{CH}_3\text{-CH}_2\text{-O}$ intermediates. Grey, yellow, red and blue spheres correspond to Rh, C, O and H atoms, respectively.

Initial state	Transition state	Final state	Activation energy (kJ/mol)	Reaction energy (kJ/mol)	Imaginary frequency (cm^{-1})	Rate constants at 300 K (s^{-1})
(a) $\text{CH}_2\text{-CH}_2\text{-O} + 2\text{H} \rightarrow \text{CH}_2\text{-CH}_2\text{-OH} + \text{H}$			35	-21	569	3.6×10^{10}
(b) $\text{CH}_2\text{-CH}_2\text{-OH} + \text{H} \rightarrow \text{CH}_3\text{-CH}_2\text{-OH}$			60	44	149	7.6×10^7
(c) $\text{CH}_2\text{-CH}_2\text{-O} + 2\text{H} \rightarrow \text{CH}_3\text{-CH}_2\text{-O} + \text{H}$			62	9	575	5.8×10^7
(d) $\text{CH}_3\text{-CH}_2\text{-O} + \text{H} \rightarrow \text{CH}_3\text{-CH}_2\text{-OH}$			118	-11	1143	573

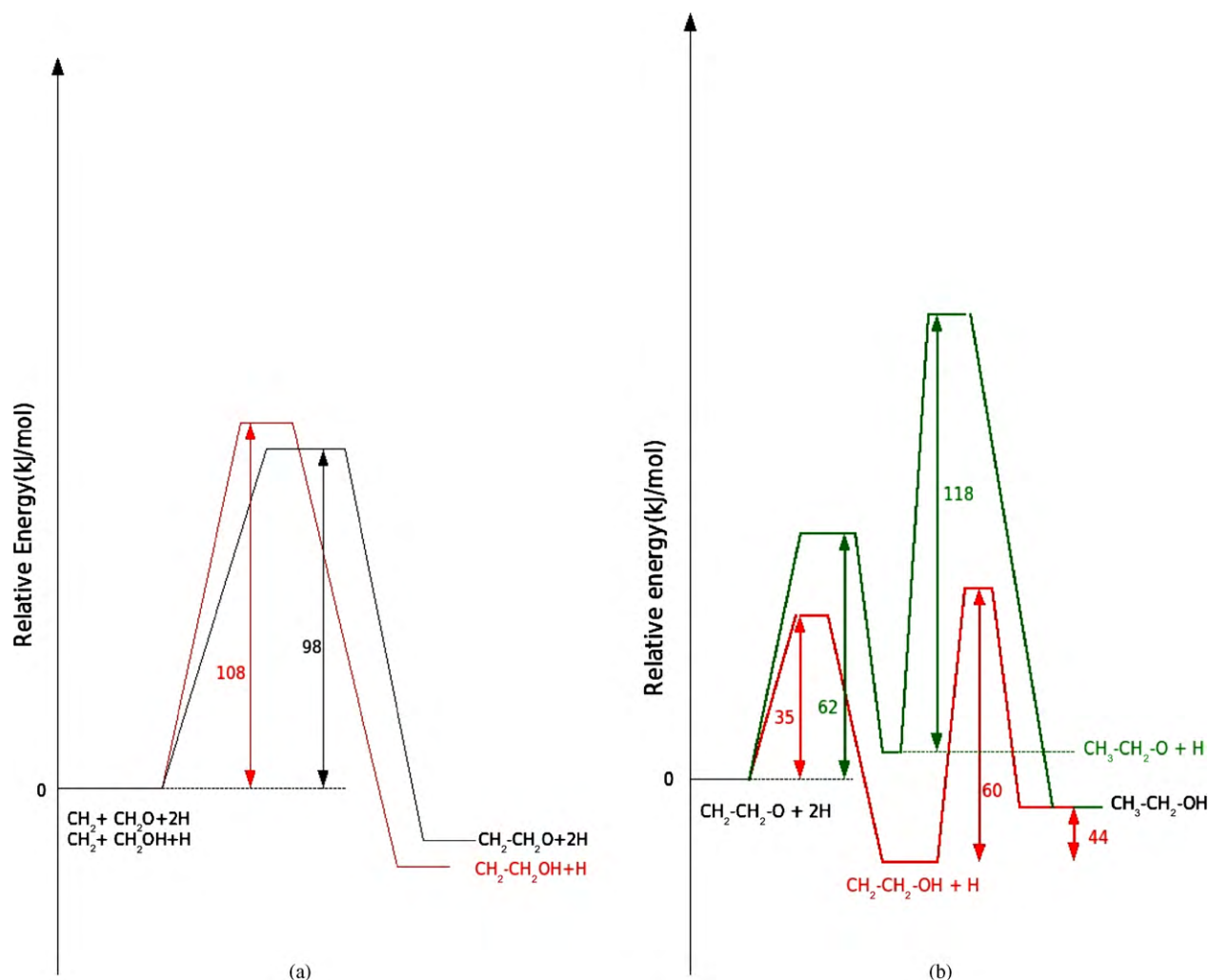


Fig. 10. Reaction paths for the C–C coupling of (a) CH_2 and CH_2O (black line) and CH_2OH (red line) and (b) formation of $\text{CH}_3\text{CH}_2\text{OH}$ from the $\text{CH}_2\text{-CH}_2\text{-O}$ in two different paths $\text{CH}_3\text{CH}_2\text{O}$ (green line) and $\text{CH}_2\text{CH}_2\text{OH}$ (red line) intermediates. (For interpretation of the references to color in the figure caption, the reader is referred to the web version of the article.)

the ethoxy intermediate to form ethanol is 118 kJ/mol. The overall barrier for ethanol formation via the ethoxy intermediate is 127 kJ/mol as shown in Fig. 10b. This is 88 kJ/mol higher than the earlier path via the hydroxyethyl intermediate. This indicates that the formation of ethanol will not proceed through an ethoxy intermediate. Interestingly, in our earlier discussion we also showed that methanol formation is not possible through the methoxy intermediate. However, one should note that the formation of CH_2 via the CH_2O intermediate requires an overall barrier of 180 kJ/mol as discussed earlier. Moreover, the low hydrogenation barriers from the CH_2O intermediate rules out the C–C coupling reaction from the CH_2O intermediates.

4. Conclusions

In the present work we investigated several reaction paths for the formation of CH_x ($x=0$ to 4) and oxygenated species such as aldehydes, acids and alcohols from syngas on a Rh_6 cluster. From this analysis we propose the following for the selectivity of the syngas conversion reaction on a Rh_6 cluster.

(1) The initial step in the formation of oxygenates from the syngas is the hydrogenation of CO to form the HCO intermediate. Interestingly this step which has been found to be the rate-

limiting step with a barrier of 123 kJ/mol for the formation of oxygenates on $\text{Rh}(1\ 1\ 1)$ surface has a lower barrier on the Rh_6 cluster corresponding to 88 kJ/mol.

- (2) The COH intermediates is a precursor state for CH_x species. However, the initial hydrogenation step to create the COH intermediate requires a barrier of 147 kJ/mol. The HCO intermediate also provides an alternative route to produce the CH_x species. The overall barrier for CO bond cleavage via the hydrogenated intermediates, i.e. COH or HCO, corresponds to around 180 kJ/mol. This overall barrier is lower than that on the $\text{Rh}(1\ 1\ 1)$ surface where it can be calculated to be more than 200 kJ/mol.
- (3) The formation of C_1 oxygenates such as CH_3OH and CH_2O proceeds via the hydrogenation of the CH_2O and HCO intermediates, respectively. The formation of CH_3OH competes with the formation of CH_4 from the CH_2OH intermediate. These results reveal that the major products on the Rh_6 cluster depend upon the reaction conditions. Under hydrogen rich conditions and normal temperatures and pressures, it would lead to methanol and methane formation while under high pressure conditions, it would result in the formation of formaldehyde. The selectivity to methanol formation depends upon the $\text{CO}:\text{H}_2$ ratio.

- (4) The formation of C₂ oxygenates take place via the CO or the COH insertion in the CH₃ intermediate. The CO insertion in the CH₃ has a barrier of 73 kJ/mol. This is about 38 kJ/mol lower than that on the Rh(1 1 1) surface. The hydrogenation of the CH₃–CO results into the acetaldehyde which has an overall barrier of 102 kJ/mol with respect to the CH₃ + CO. This is about 46 kJ/mol lower than that on Rh(1 1 1) surface. The other reaction is the formation of acetic acid via OH insertion in CH₃CO with a barrier of 115 kJ/mol. Ethanol formation proceeds via the CH₃–COH intermediate followed by hydrogenation steps. The overall barrier from the CH₃ and COH intermediate for the formation of ethanol is 173 kJ/mol. This is about 26 kJ/mol lower than that on the Rh surface where the overall barrier is reported to be 199 kJ/mol. The main conclusion for the syngas conversion on the Rh₆ cluster is that the CO bond dissociation which requires a high barrier of around 180 kJ/mol will not be a feasible route to produce several CH_x species which couple to form hydrocarbons. However, the CO, COH or HCO insertion in the CH_x species will be the optimum paths for the production of oxygenated compounds on Rh₆ cluster. The overall barriers required to produce the oxygenated compounds on Rh₆ cluster are lower than that on the Rh surface.

Acknowledgements

S. Shetty and R. A. van Santen would like to thank the National Computing Facility (NCF) for the computational facilities (Grant: SH-114). The authors gratefully acknowledge Dr. Steven W. Levine (ExxonMobil) for his support and valuable comments to improve the quality of this manuscript.

Appendix A. Supplementary data

Supplementary data associated with this article can be found, in the online version, at doi:10.1016/j.molcata.2010.07.004.

References

- [1] (a) F. Fischer, H. Tropsch, *Brennst. Chem.* 4 (1923) 276;
(b) R.B. Anderson, *The Fischer–Tropsch Synthesis*, Academic Press, New York, 1984;
(c) G.A. Somorjai, *Introduction to surface Chemistry and Catalysis*, Wiley, New York, 1994;
- (c) A.P. Stynberg, M.E. Dry, *Fischer–Tropsch Technology on Studies of Surface Science and Catalysis*, Elsevier, 2004.
- [2] (a) M.A. Vannice, *J. Catal.* 50 (1977) 228;
(b) R.D. Kelley, D.W. Goodman, *The Chemical Physics of Solid Surface and Heterogeneous Catalysis*, Elsevier, Amsterdam, 1982.
- [3] J.J. Spivey, A. Egbebi, *Chem. Soc. Rev.* 36 (2007) 1514.
- [4] R.A. van Santen, M. Neurock, *Molecular Heterogeneous Catalysis*, Wiley-VCH, Weinheim, 2006.
- [5] M.L. Turner, N. Marsih, B.E. Mann, R. Quayom, H.C. Matilis, P.M. Long, *J. Am. Chem. Soc.* 124 (2002) 10456.
- [6] O.R. Inderwildi, S.J. Jenkins, D.A. King, *J. Phys. Chem. C* 112 (2008) 1305.
- [7] R.G. Herman, in: L. Guzzi (Ed.), *Studies of Surface Science and Catalysis*, 1991, p. 265.
- [8] P. Matilis, *J. Mol. Catal.* 204 (2003) 54.
- [9] A. Farrell, R.J. Plevin, B. Turner, A.D. Jones, M. O'Hare, D.M. Kammen, *Science* 311 (2006) 506.
- [10] M.A. Haider, M.R. Gogate, R.J. Davis, *J. Catal.* 261 (2009) 9.
- [11] M.M. Bhasin, W.J. Bartley, P.C. Ellgen, T.P. Wilson, *J. Catal.* 54 (1978) 120.
- [12] J. Guzman, B.C. Gates, *B.C. Dalton, Transactions* (2003) 3303.
- [13] Y. Wang, H. Luo, D. Liang, X. Bao, *J. Catal.* 196 (2000) 46.
- [14] X. Pan, Z. Fan, W. Chen, Y. Ding, H. Luo, X. Bao, *Nature* 6 (2007) 507.
- [15] W.M.H. Sachtler, M. Ichikawa, *J. Phys. Chem.* 90 (1986) 4752.
- [16] S.S.C. Chuang, R.W. Stevens Jr., R. Khatri, *Top. Catal.* 32 (2005) 225.
- [17] D. Mei, R. Rousseau, S.M. Kathmann, V.-A. Glezakou, M.H. Engelhard, W. Jiang, C. Wang, M.A. Gerber, J.F. White, D.J. Stevens, *J. Catal.* 271 (2010) 325.
- [18] Y.M. Choi, P. Liu, *J. Am. Chem. Soc.* 131 (2009) 13054.
- [19] L.-F. Rao, A. Fukuoka, M. Ichikawa, *J. Chem. Soc. Chem. Commun.* (1988) 459.
- [20] T.J. Lee, B.C. Gates, *Catal. Lett.* 8 (1991) 15.
- [21] (a) G. Kresse, J. Hafner, *Phys. Rev. B* 49 (1994) 14251;
(b) G. Kresse, J. Furthmuller, *Comput. Mater. Sci.* 6 (1996) 15.
- [22] (a) P.E. Blochl, *Phys. Rev. B* 50 (1994) 17953;
(b) G. Kresse, J. Joubert, *Phys. Rev. B* 59 (1999) 1758.
- [23] G. Henkelman, H. Jónsson, *J. Chem. Phys.* 113 (2000) 9978.
- [24] K.J. Laidler, *Theories of Chemical Reaction Rates*, McGraw-Hill, New York, 1969.
- [25] M.P. Andersson, F. Abild-Pedersen, I.N. Remediakis, T. Bligaard, G. Jones, J. Engbaek, O. Lytken, S. Horch, J.H. Nielsen, J. Sehested, J.R. Rostrup-Nielsen, J.K. Nørskov, I. Chorkendorf, *J. Catal.* 255 (2008) 6.
- [26] S. Shetty, S. Strych, A.P.J. Jansen, R.A. van Santen, *Can. J. Chem.* 87 (2009) 824.